

---

# COARSE-GRAINING BISTABILITY WITH THE MARTINI FORCE FIELD \*

---

Alexander D. Muratov, Vladik A. Avetisov

Semenov Federal Research Center for Chemical Physics, Russian Academy of Sciences, 119991 Moscow, Russia  
Design Center for Molecular Machines, Moscow, Russia  
alexander.muratov@chph.ras.ru (A.D.M.); avetisov@chph.ras.ru (V.A.A.);

## ABSTRACT

An increasing interest in molecular structures whose long term dynamics resemble those of bistable mechanical systems promotes the search of possible candidates that may operate as two-state switching units. Of particular interest are the systems that are capable to exhibit such bistable effects as spontaneous vibrations, stochastic resonance and spontaneous synchronization. Previously, in all-atom molecular dynamics simulations it has been demonstrated that short pyridine-furan springs show these bistable phenomena. In this article we introduce a coarse-grained model of such springs and investigate the possibility to observe the bistability effects, such as spontaneous vibrations. Our findings allow the studies of short pyridine-furan springs at large time and length scales and open field for further computational research of large bistable systems.

**Keywords** Bistability · nanosprings · non-linear dynamics · spontaneous vibrations · stochastic resonance · coarse-grained molecular dynamics · Martini

## 1 Introduction

The growing attention to nanoscale molecular structures with the dynamics reminiscent of the bistable mechanical systems is driven by the increasing demand for the development and implementation of various nanodevices. These devices may act as switches and logic gates[1, 2, 3, 4, 5, 6], sensors and actuators[7, 8, 9, 10, 11, 12], as well as mechano-electrical converters[13, 14] and energy harvesters[15, 16, 17, 18]. Nanoscale bistable systems are equally important for validating the principles of stochastic thermodynamics[19, 20, 21, 22]. The field is currently focused on expanding thermodynamic theories to include nanoscale molecular machines[21, 23, 24, 25, 26].

This article introduces a coarse-grained model of spiral-like compound, pyridine-furan (PF), which consists of 6- and 5-member hetherocycles (consult Figure 1(a)), containing nitrogen and oxygen respectively[27, 28]. This copolymer tends to form a helical shape stabilized by the interaction of  $\pi$ -electrons between neighboring turns, as shown by quantum calculations[29]. Our previous modeling reveals that oligo-PF springs exhibit bistable dynamics of Duffing oscillators, accompanied by spontaneous vibrations and stochastic resonance activated by thermal fluctuations[30, 31]. Moreover, dynamical synchronization of two or several oligo-PF springs is also possible[32]. Nevertheless, a raise in the number of synchronized oligo-PF springs inevitably leads to the increase of the simulation box and subsequently to the slower simulation times. Moreover, our theoretical findings suggest an increase of lifetime of oligo-PF springs in each bistable state. Thus if we desire to simulate synchronization of a large number of oligo-PF springs, we have to compute more time steps while each time step is calculated slower, making all-atom modeling almost impossible. An easy and elegant way to overcome this issue is coarse-graining (CG). There are two approaches to the CG modeling: "bottom-up," which concentrates on accurately representing the underlying atomic structure of the compound, and "top-down," which focuses on reproduction of macroscopic properties of the compound. The main disadvantage of "bottom-up" models, despite their accuracy, is their non-transferability; that is, re-parameterization is required whenever modeling conditions change. Also, they often use complex potential forms that slow down calculations. At the same

---

\* Citation: A.D.Muratov and V.A.Avetisov, Title. Pages.... DOI:000000/11111.

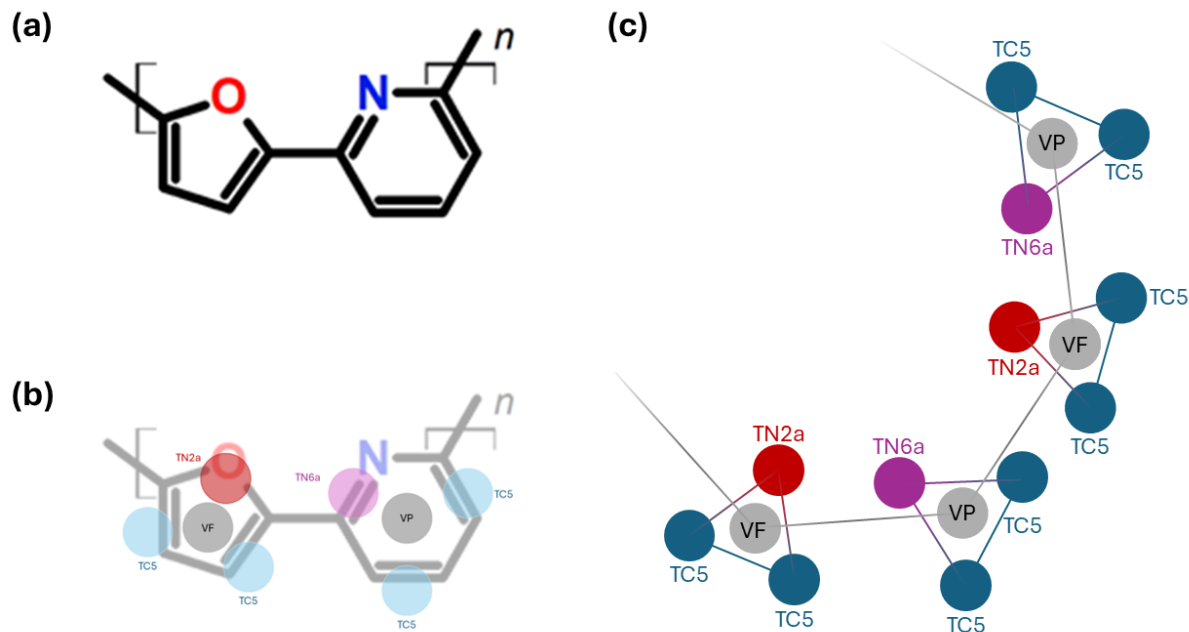


Figure 1: Pyridine-furan (PF) spring with five monomer units (oligo-PF-5 spring): (a) Chemical structure of a pyridine-furan monomer unit with heterocyclic rings in cis-configuration. (b) Mapping scheme of oligo-PF spring. (c) Two coarse-grained monomer units of oligo-PF spring.

time, "top-down" approaches use simple potential forms and usually make use of the idea of pre-parameterized building blocks, making them easily transferable and computationally cheap.

Among various "top-down" CG force fields stand out Martini (which usually deciphers as MARrink Toolkit Initiative) that uses water/oil partitioning free energy to parameterize Lennard-Jones (LJ) potentials[33, 34]. The keystone of the Martini force field is several discrete interaction levels between a limited number of building blocks. First introduced for lipids[33], later it has been updated to include more compounds in its second version[34] including proteins[35], carbohydrates[36], DNA[37] and various other compounds. Recently, a new version, coined Martini 3, with improved accuracy has been released[38, 39]. The main difference is the introduction of so-called "tiny" particles; this improvement plays a significant role for more accurate description of ring structures. Thus, picking Martini 3 for oligo-PF springs seems to be a straightforward choice.

In this paper we introduce a coarse-grained model of the oligo-PF spring within the latest version of Martini force field. The model captures the bistable dynamic effects of these oligo-PF springs with thermally-activated spontaneous vibrations and stochastic resonance.

## 2 Materials and Methods

### 2.1 Non-bonded parameterization

Martini 3 incorporates four main types of beads: charged (Q), polar (P), non-polar (N) and apolar (C). There are also special beads for water (W), divalent ions (D) and groups containing halogen atoms (X). Most bead types except for W-bead type and D-bead type are divided in subtypes. For the simplicity, the LJ interaction levels  $\epsilon$  are discretized; there are 22 possible interaction levels. Sizes of the beads  $\sigma$  are also discretized in Martini 3: there are regular (R,  $\sigma = 0.47$  nm), small (S,  $\sigma = 0.41$  nm) and tiny (T,  $\sigma = 0.34$  nm) beads. These beads are intended to be used for 4-to-1, 3-to-1 and 2-to-1 mappings respectively. Both pyridine and furan are already parameterized within Martini 3 force field[39], and more thorough discussion will follow in the next subsection 2.2. Water is represented by a regular W bead.

## 2.2 Bonded parameterization

Aromatic ring structures are well-described by three T-beads:  $(TC5)_2$ -TN2a is a representation for furan and  $(TC5)_2$ -TN6a - for pyridine (TN2a bead includes oxygen, TN6a - nitrogen; consult Figure 1(b-c) for more details). It is important to emphasize that in furan TN2a bead shares  $-CH-$  groups with neighboring TC5 beads, while in pyridine beads does not share atomic groups (see Figure 1(b))[39]. Alessandri et al. [39] determined bonded parameters for standalone pyridine and furan, but bond lengths will differ in compound. Here, an important difference from the previous issue of Martini is that center of each bead corresponds to the center of geometry (COG) of underlying molecular structure rather than center of mass (COM). This is especially relevant for tiny beads.

To obtain bond potentials within the oligo-PF-5 molecule we adopt a strategy for long chains of rigid fragments called "Divide and Conquer"[39, 40]. Within this strategy we introduce a virtual dummy site (mass-less and not interacting via non-bonded interactions) at the center of geometry of each pyridine or furan ring. Then, we connect them with an harmonic bond and exclude the nonbonded interactions between the two rings (see Figure 1(c)). Valence angle potentials, such as  $V_i-V_j-V_k$ ,  $B_{i1}-V_i-V_j$  or  $B_{i2}-B_{i3}-V_j$  where  $V_i$ ,  $V_j$  and  $V_k$  are the  $i$ -th,  $j$ -th and  $k$ -th virtual sites and  $B_{i1}$ ,  $B_{i2}$ ,  $B_{i3}$  are the beads of the  $i$ -th ring, may also be introduced (here for  $B_{i1}$  it is convenient to take the bead describing oxygen/nitrogen; consult Figure 1(c) for more details). Last, a dihedral potential  $B_{i1}-V_i-V_j-B_{j1}$  can be directly applied in such a construction.

## 2.3 Computational details

For modeling we use Gromacs 2023[41] with the number of particles, volume and temperature maintained constant (NVT) ensemble. The temperature is set to 298 K and maintained by a velocity-rescale thermostat[42] with 1.0 ps coupling time. For parameterization we perform 10 ns atomistic simulations of oligo-PF-5 spring using OPLS-AA[43] force field parameters for the oligomer, and the SPC/E model[44] for water. After obtaining atomistic trajectories, we calculate reference probability distributions for valence bonds and valence angles and get initial CG potentials, which are used for a primary 25 ns CG simulation run; then we compare CG probability distributions with reference ones. We keep changing CG potentials until reasonable convergence between probability distributions is obtained. For CG calculations we use straight cutoff LJ potential that turns to zero at 1.1 nm[45].

To study the bistable dynamics of the oligo-PF-5, we fixed one end of the spring, while a pulling force was applied along the axis of the spring to another end of the spring. The distance (denoted  $R_e$ ) between the ends of the oligo-PF-5 spring was considered a collective variable describing the long-term dynamics of the spring. Bistability of the oligo-PF-5 spring was specified in the agreement with two well-reproduced states of the spring with the end-to-end distances equal to  $R_e \sim 0.4$  nm and  $R_e \sim 0.75$  nm. These states are referred to as the squeezed and the stress-strain states, respectively.

## 3 Results

### 3.1 Non-bonded and bonded interactions

As mentioned in subsections 2.1 and 2.2, both pyridine and furan are already parameterized in Martini 3, but bonded potentials in a conjugated compound differ from those in a single heterocycle. To obtain these potentials, we first perform 10 ns atomistic simulations of oligo-PF-5 using OPLS-AA force field with NVT ensemble. Temperature is maintained by velocity-rescale thermostat with 1.0 ps coupling time. Then, we calculate probability distributions for all possible bonds and valence angles and thus get primary CG potentials which are then used for a trial run. The probabilities got from atomistic trajectory serve as target ones. We keep modifying CG potentials until the centers and widths of the distributions correspond the target ones. The obtained values are given in Table 1

Since in pyridine atomic groups are not shared between beads, an asymmetry is observed in certain pairs of valence angles: TN6a- $V_P$ - $(*)V_F$  and  $V_F$ - $(*)V_P$ - $(*)TN6a$  or TC5p-TC5p- $(*)V_F$  and  $V_F$ - $(*)TC5p$ - $(*)TC5p$  (consult Figure 1(b) for more details). Also, a dihedral potential TN6a- $V_P$ - $(*)V_F$ - $(*)TN2a$  is directly taken from OPLS-AA force field.

### 3.2 Spontaneous vibrations

To investigate the dynamics of the CG oligo-PF-5 spring under tension, we followed the same strategy as for all-atom model[30]. After equilibrating the oligo-PF-5 spring at 298 K with one end fixed and applying a force  $\vec{F}$  along the spring axis to pull the other end, the spring's initial state remained stable under weak tensile conditions. However, once the pulling force reached a specific critical value, approximately  $F_c = 100$  pN, the oligo-PF-5 spring began to exhibit spontaneous vibrations between squeezed state and stress-strain state. The average end-to-end distances of the spring

Table 1: Intramolecular potentials of oligo-PF-5. Here, subscripts <sub>F</sub> and <sub>P</sub> denote belonging to furan and pyridine. An asterisk (\*) denotes a bead from neighboring ring

Valence bond	$r_0$ , nm	$k_b$ , kJ mol <sup>-1</sup> nm <sup>-2</sup>	Valence angle	$\theta_0$	$k_\theta$ , kJ mol <sup>-1</sup>
TN2a-TC5 <sub>F</sub>	0.1765	rigid	V <sub>F</sub> -V <sub>P</sub> -V <sub>F</sub>	120	1500
TC5 <sub>F</sub> -TC5 <sub>F</sub>	0.2125	rigid	V <sub>P</sub> -V <sub>F</sub> -V <sub>P</sub>	132	1500
TN6a-TC5 <sub>P</sub>	0.25	rigid	TN2a-V <sub>F</sub> -(*)V <sub>P</sub>	67	1000
TC5 <sub>P</sub> -TC5 <sub>P</sub>	0.255	rigid	TN6a-V <sub>P</sub> -(*)V <sub>F</sub>	80	1000
V <sub>F</sub> -V <sub>P</sub>	0.438	50000	V <sub>F</sub> -(*)V <sub>P</sub> -(*)TN6a	40	1000
			TC5 <sub>P</sub> -TC5 <sub>P</sub> -(*)V <sub>F</sub>	161	500
			V <sub>F</sub> -(*)TC5 <sub>P</sub> -(*)TC5 <sub>P</sub>	110	500
			TC5 <sub>F</sub> -TC5 <sub>F</sub> -(*)V <sub>P</sub>	145	500

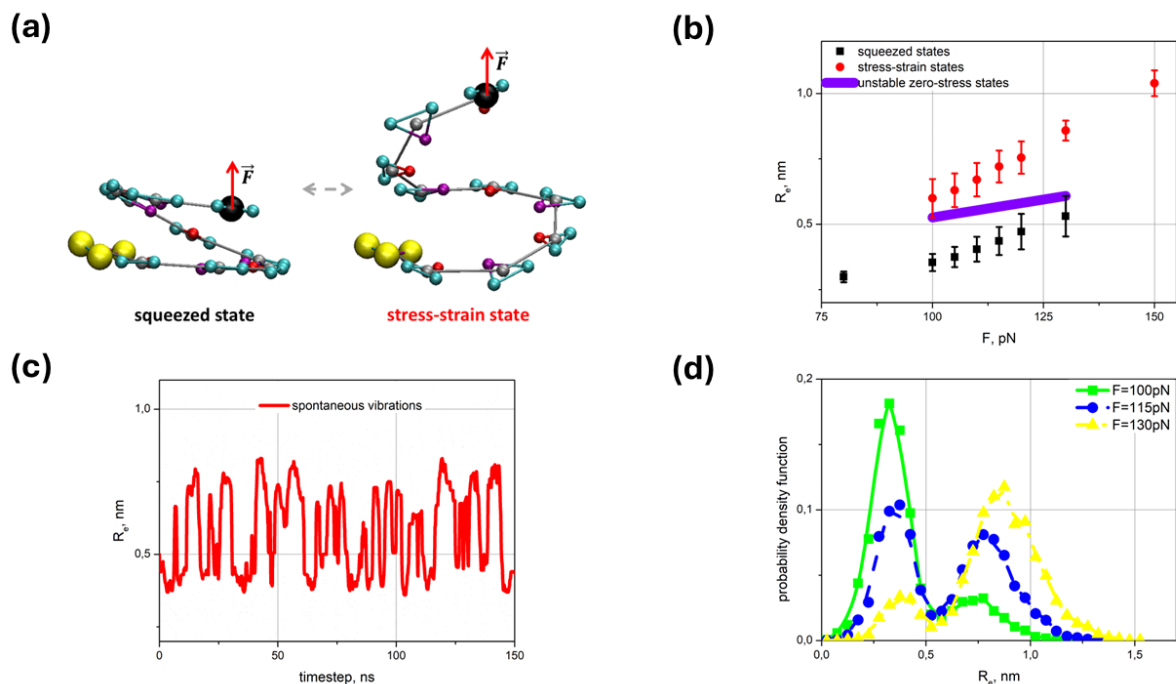


Figure 2: (a) Coarse-grained model of the oligo-PF-5 system with a pulling force. The squeezed and the stress-strain states of the spring are shown on the left and right, respectively. The yellow spheres at the lower end of the spring indicate the fixation of the pyridine ring by rigid harmonic force. The pulling force,  $F$ , is applied to the top end of the spring. (b) The state diagram shows a linear elasticity of oligo-PF-5 spring up to  $F \approx 100$  pN and bistability of the spring in the region from  $F \approx 100 - 130$  pN; (c) Spontaneous vibrations of the oligo-PF-5 spring at  $F \approx 115$  pN; (d) Evolution of the probability density for the squeezed and stress-strain states when pulling force surpasses the critical value.

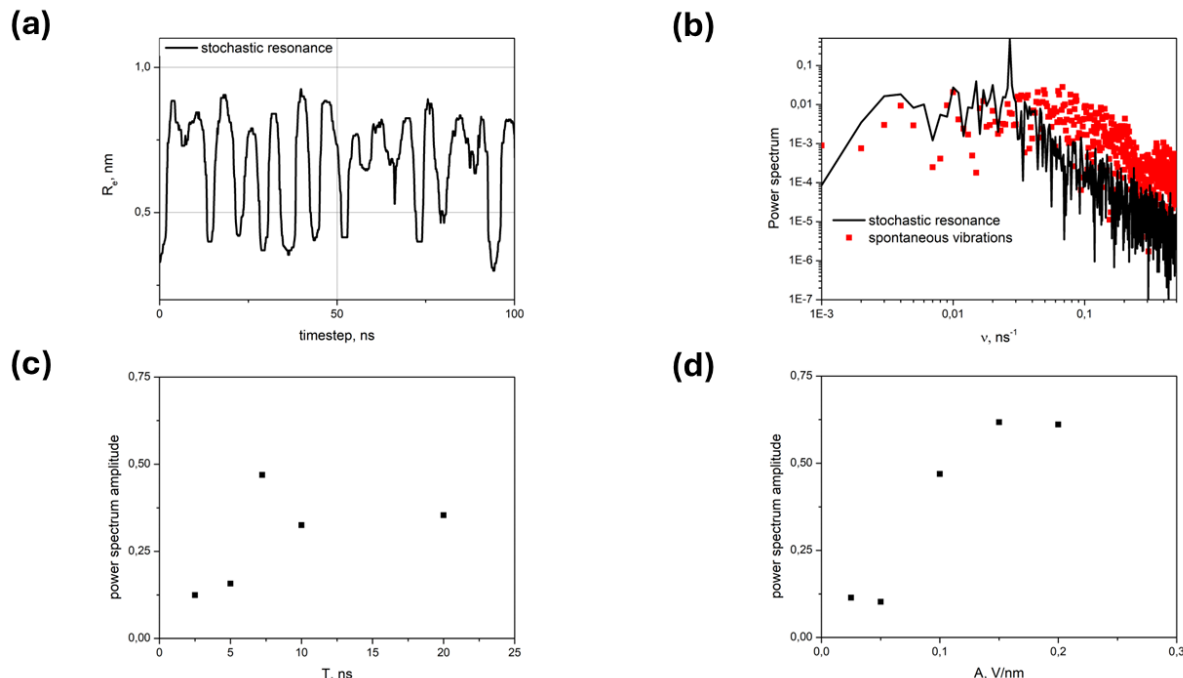


Figure 3: Stochastic resonance of the oligo-PF-5 induced by an oscillating field  $E = E_0 \cos(2\pi\nu t) = E_0 \cos(2\pi t/T)$ : (a) The dynamic trajectory at  $F = 115$  pN,  $T = 7.5$  ns, and  $E_0 = 0.2$  V nm<sup>-1</sup>; (b) Power spectrum of spontaneous vibrations (red curve) and stochastic resonance (black curve); (c) The dependence of the main resonance peak amplitude on the period  $T$  of oscillating field ( $E_0 = 0.1$  V nm<sup>-1</sup>); (d) The dependence of the main resonance peak amplitude on  $E_0$  ( $T_0 = 7.2$  ns).

between the states differ by approximately 0.35 nm, which is in accordance with both *abinitio* calculations[29] and atomistic simulations. Figure 2a) displays coarse-grained level snapshots of these two states.

The evolution of the statistics of visits to the squeezed and stress-strain states as the pulling force exceeds the critical point  $F_c$  is shown on Figures 2(b,d). Within the range of  $F = 110 - 120$  pN, both the squeezed and stress-strain states are visited almost equally. The mean lifetimes of the states in the spontaneous vibration mode differed in the bistability region, ranging from  $\tau = 1 - 30$  ns, depending on the tensile force. In the symmetrical bistability region, neither the squeezed state nor the stress-strain state dominates, resulting in the mean lifetimes of the two states being approximately equal to  $\tau = 3.6$  ns. Figure 2(c) illustrates a typical trajectory of the long-term dynamics  $R_e(t)$  of the oligo-PF-5 spring within the symmetrical bistability region. Clear spontaneous vibrations of the spring can be observed without any additional random perturbations being applied to activate them. These vibrations are activated only by the fluctuations of the thermal bath; on the other hand, outside the bistability region, trajectories without vibrations prevail.

### 3.3 Stochastic resonance

We examined the stochastic resonance mode of the oligo-PF-5 spring by applying an additional oscillating force that acted weakly on the pulling end of the spring. This force was modeled by the application of an oscillating electrical field,  $E = E_0 \cos(2\pi\nu t)$ , on a unit charge preset on the pulling end of the spring. Since CG particles are uncharged, such an addition should not affect the dynamics of the system. Typical vibrations of the end-to-end distance of the oligo-PF-5 spring in the stochastic resonance mode and the power spectrum of the vibrations are shown in Figures 3(a-b).

According to the stochastic resonance theory[46, 47], the main resonance peak was observed at the frequency  $\nu = (2\tau)^{-1}$ , that is, the period of the applied oscillating field was equal to twice the mean lifetime of the state in the spontaneous vibrations mode. In fact, we scanned a wide range of oscillating fields to find the maximal resonance response defined in terms of the spectral component at the resonance frequency. Corresponding results are presented in Figure 3(c,d). Regarding the amplitude of the oscillating field, the maximum resonance was found for  $E_0 = 0.2$  V nm<sup>-1</sup> in full accordance with the all-atom data[30]. It should be noted that outside the symmetric bistability region, the

lifetimes of the squeezed and the stress–strain states became so different that the average lifetime was no longer a good guide to the resonance frequency, and thus the resonance response was screened in the region of symmetric bistability at  $F = 115$  pN.

## 4 Discussion

The main finding of this work is that subtle bistable effects, such as spontaneous vibrations and stochastic resonance, can be observed using coarse-grained molecular dynamics. Indeed, our previous studies suggest that spontaneous vibrations arise due to  $\pi$ -stacking between aromatic groups located on the adjacent turns of the spring, which along with the stiffness of the molecular backbone produces a two-well potential (see Avetisov et al. [30] for more information). One can speculate how can  $\pi$ -stacking be addressed in molecular dynamics (authors may suppose that it somehow emerges due to a peculiar interplay between Lennard-Jones forces and Coulomb interaction of the partial charges of the atoms of the rings, but such question is very far out of the scope of the current work), but in the present Martini model adjacent turns of the spring interact exclusively via LJ potential. In the meantime, chain stiffness is kept by bonding between virtual dummy particles; both factors seem strong arguments against observing bistability. Thus, such emerging noticeably strengthens the credibility of Martini force field and provides for its wider usability for the molecular modeling field.

Still, there is a certain difference between spontaneous vibrations observed in the present work and in our previous atomistic modeling[30]. In CG modeling, SV occur at smaller forces: 100–120 pN compared with 270–290 pN for all-atom modeling. Nevertheless, we do not think it should be considered as significant disadvantage of the model: the fact that the mean lifetimes in the states 1–30 ns correspond to those obtained in fully atomic simulation and that the widths of the force regions coincide seems to be more important.

For the present work we have taken pre-parameterized pyridine and furan[39] and as a consequence have determined only bonded potentials. Since TN2a bead in furan shares -CH- group with adjacent TC5 beads while in pyridine beads does not share molecular groups with their neighbors, we are obliged to introduce differing valence angle potentials (for instance, TN6a-V<sub>P</sub>-(\*)V<sub>F</sub> and V<sub>F</sub>-(\*)V<sub>P</sub>-(\*)TN6a) due to asymmetry of the resulting construction. This could be overridden by a slight re-parameterization of pyridine: if TN6a/TC5 beads representing pyridine shared -CH- groups, the construction would be symmetrical and valence angle potentials would be the same. We plan to investigate more possible mappings in our further work.

In our previous work concerning Martini[48] we noticed the ambiguity in relation to bead sizes. Fortunately, Martini 3 has addressed the issues we mentioned by introducing tiny beads and strict definition when small and tiny beads are to be used[38]. The latter preserves flexibility while implying more accuracy.

## 5 Conclusion

We have performed coarse-grained simulations of oligo-PF-5 springs subject to stretching and observed thermally-activated spontaneous vibrations and stochastic resonance. We explored the conditions under which these effects are present, indicated symmetrical bistability and determined mean lifetime of the states. The results are in good accordance with atomistic simulations. Our findings approve Martini force field as capable tool for molecular modeling. Its combined flexibility and accuracy allows its applying for the modeling of molecular machines since it is able to capture the necessary time- and lengthscales.

## Acknowledgments

Authors thank Alexey Astakhov, Vladimir Bochenkov, Maria Frolkina, Vladislav Petrovskii, Anastasia Markina and Alexander Valov for helpful discussions.

## References

- [1] Alexis Peschot, Chuang Qian, and Tsu-Jae King Liu. Nanoelectromechanical switches for low-power digital computing. *Micromachines*, 6(8):1046–1065, 2015.
- [2] Shaji Varghese, Johannes A. A. W. Elemans, Alan E. Rowan, and Roeland J. M. Nolte. Molecular computing: paths to chemical turing machines. *Chem. Sci.*, 6:6050–6058, 2015.

- [3] Sundus Erbas-Cakmak, Safacan Kolemen, Adam C. Sedgwick, Thorfinnur Gunnlaugsson, Tony D. James, Juyoung Yoon, and Engin U. Akkaya. Molecular logic gates: the past, present and future. *Chem. Soc. Rev.*, 47:2228–2248, 2018.
- [4] Lorien Benda, Benjamin Doistau, Caroline Rossi-Gendron, Lise-Marie Chamoreau, Bernold Hasenknopf, and Guillaume Vives. Substrate-dependent allosteric regulation by switchable catalytic molecular tweezers. *Communications Chemistry*, 2(1):1–11, 2019.
- [5] Guilherme B. Berselli, Aurélien V. Gimenez, Alexandra O’Connor, and Tia E. Keyes. Robust Photoelectric Biomolecular Switch at a Microcavity-Supported Lipid Bilayer. *ACS Applied Materials & Interfaces*, 13(24):29158–29169, 2021.
- [6] Federico Nicoli, Erica Paltrinieri, Marina Tranfić Bakić, Massimo Baroncini, Serena Silvi, and Alberto Credi. Binary logic operations with artificial molecular machines. *Coordination Chemistry Reviews*, 428:213589, 2021.
- [7] Liang Zhang, Vanesa Marcos, and David A. Leigh. Molecular machines with bio-inspired mechanisms. *Proceedings of the National Academy of Sciences*, 115(38):9397–9404, 2018.
- [8] Tong Shu, Qiming Shen, Xueji Zhang, and Michael J. Serpe. Stimuli-responsive polymer/nanomaterial hybrids for sensing applications. *Analyst*, 145(17):5713–5724, 2020.
- [9] Max C. Lemme, Stefan Wagner, Kangho Lee, Xuge Fan, Gerard J. Verbiest, Sebastian Wittmann, Sebastian Lukas, Robin J. Dolleman, Frank Niklaus, Herre S. J. van der Zant, Georg S. Duesberg, and Peter G. Steeneken. Nanoelectromechanical Sensors Based on Suspended 2D Materials. *Research*, 2020, 2020.
- [10] Zhao-Tao Shi, Qi Zhang, He Tian, and Da-Hui Qu. Driving Smart Molecular Systems by Artificial Molecular Machines. *Advanced Intelligent Systems*, 2(5):1900169, 2020.
- [11] Ivan Aprahamian. The Future of Molecular Machines. *ACS Central Science*, 6(3):347–358, 2020.
- [12] Yinding Chi, Yanbin Li, Yao Zhao, Yaoye Hong, Yichao Tang, and Jie Yin. Bistable and multistable actuators for soft robots: Structures, materials, and functionalities. *Advanced Materials*, 34(19):2110384, 2022.
- [13] C. Dutreix, R. Avriller, B. Lounis, and F. Pistolesi. Two-level system as topological actuator for nanomechanical modes. *Physical Review Research*, 2(2):023268, 2020.
- [14] Yunteng Cao, Masoud Derakhshani, Yuhui Fang, Guoliang Huang, and Changyong Cao. Bistable structures for advanced functional systems. *Advanced Functional Materials*, 31(45):2106231, 2021.
- [15] Huidong Li, Chuan Tian, and Z. Daniel Deng. Energy harvesting from low frequency applications using piezoelectric materials. *Applied Physics Reviews*, 1(4):041301, 2014.
- [16] Shi Hyeong Kim, Márcio D. Lima, Mikhail E. Kozlov, Carter S. Haines, Geoffrey M. Spinks, Shazed Aziz, Changsoon Choi, Hyeon Jun Sim, Xuemin Wang, Hongbing Lu, Dong Qian, John D. W. Madden, Ray H. Baughman, and Seon Jeong Kim. Harvesting temperature fluctuations as electrical energy using torsional and tensile polymer muscles. *Energy & Environmental Science*, 8(11):3336–3344, 2015.
- [17] M. L. Ackerman, P. Kumar, M. Neek-Amal, P. M. Thibado, F. M. Peeters, and Surendra Singh. Anomalous Dynamical Behavior of Freestanding Graphene Membranes. *Physical Review Letters*, 117(12):126801, 2016.
- [18] P. M. Thibado, P. Kumar, Surendra Singh, M. Ruiz-Garcia, A. Lasanta, and L. L. Bonilla. Fluctuation-induced current from freestanding graphene. *Physical Review E*, 102(4):042101, 2020.
- [19] Denis J. Evans and Debra J. Searles. The Fluctuation Theorem. *Advances in Physics*, 51(7):1529–1585, 2002.
- [20] Udo Seifert. Stochastic thermodynamics, fluctuation theorems and molecular machines. *Reports on Progress in Physics*, 75(12):126001, 2012.
- [21] S. Ciliberto. Experiments in Stochastic Thermodynamics: Short History and Perspectives. *Physical Review X*, 7:021051, 2017.
- [22] Jordan M. Horowitz and Todd R. Gingrich. Thermodynamic uncertainty relations constrain non-equilibrium fluctuations. *Nature Physics*, 16(1):15–20, 2020.
- [23] G. M. Wang, E. M. Sevick, Emil Mittag, Debra J. Searles, and Denis J. Evans. Experimental Demonstration of Violations of the Second Law of Thermodynamics for Small Systems and Short Time Scales. *Physical Review Letters*, 89(5):050601, 2002.
- [24] P. Jop, A. Petrosyan, and S. Ciliberto. Work and dissipation fluctuations near the stochastic resonance of a colloidal particle. *EPL (Europhysics Letters)*, 81(5):50005, 2008.
- [25] R. D. Astumian. Stochastic pumping of non-equilibrium steady-states: how molecules adapt to a fluctuating environment. *Chemical Communications*, 54(5):427–444, 2018.

- [26] Hadrien Vroylandt, Massimiliano Esposito, and Gatiën Verley. Efficiency Fluctuations of Stochastic Machines Undergoing a Phase Transition. *Physical Review Letters*, 124(25):250603, 2020.
- [27] R. Alan Jones, Marielena Karatza, Tevita N. Voro, Pervin U. Civeir, Annete Franck, Orhan Ozturk, John P. Seaman, Alexander P. Whitmore, and David J. Williamson. Extended heterocyclic systems 1. the synthesis and characterisation of pyrrolylpyridines, alternating pyrrole: Pyridine oligomers and polymers, and related systems. *Tetrahedron*, 52(26):8707–8724, 1996.
- [28] R. Alan Jones and Pervin U. Civeir. Extended heterocyclic systems 2. the synthesis and characterisation of (2-furyl) pyridines, (2-thienyl) pyridines, and furan-pyridine and thiophene-pyridine oligomers. *Tetrahedron*, 53(34):11529–11540, 1997.
- [29] Harikrishna Sahu, Shashwat Gupta, Priyank Gaur, and Aditya N. Panda. Structure and optoelectronic properties of helical pyridine–furan, pyridine–pyrrole and pyridine–thiophene oligomers. *Physical Chemistry Chemical Physics*, 17(32):20647–20657, 2015.
- [30] Vladik A. Avetisov, Maria A. Frolkina, Anastasia A. Markina, Alexander D. Muratov, and Vladislav S. Petrovskii. Short pyridine-furan springs exhibit bistable dynamics of duffing oscillators. *Nanomaterials*, 11(12), 2021.
- [31] Alexey M. Astakhov, Vladislav S. Petrovskii, Maria A. Frolkina, Anastasia A. Markina, Alexander D. Muratov, Alexander F. Valov, and Vladik A. Avetisov. Spontaneous vibrations and stochastic resonance of short oligomeric springs. *Nanomaterials*, 14(1):41, 2024.
- [32] Anastasia A. Markina, Maria A. Frolkina, Alexander D. Muratov, Vladislav S. Petrovskii, Alexander F. Valov, and Vladik A. Avetisov. Spontaneous Synchronization of Two Bistable Pyridine-Furan Nanosprings Connected by an Oligomeric Bridge. *Nanomaterials*, 14(1):3, 2023.
- [33] Siewert J. Marrink, Alex H. de Vries, and Alan E. Mark. Coarse Grained Model for Semiquantitative Lipid Simulations. *The Journal of Physical Chemistry B*, 108(2):750–760, 2004.
- [34] Siewert J. Marrink, H. Jelger Risselada, Serge Yefimov, D. Peter Tieleman, and Alex H. de Vries. The MARTINI Force Field: Coarse Grained Model for Biomolecular Simulations. *The Journal of Physical Chemistry B*, 111(27):7812–7824, 2007.
- [35] Luca Monticelli, Senthil K. Kandasamy, Xavier Periole, Ronald G. Larson, D. Peter Tieleman, and Siewert-Jan Marrink. The MARTINI Coarse-Grained Force Field: Extension to Proteins. *Journal of Chemical Theory and Computation*, 4(5):819–834, 2008.
- [36] Cesar A. López, Andrzej J. Rzepiela, Alex H. de Vries, Lubbert Dijkhuizen, Philippe H. Hünenberger, and Siewert J. Marrink. Martini Coarse-Grained Force Field: Extension to Carbohydrates. *Journal of Chemical Theory and Computation*, 5(12):3195–3210, 2009.
- [37] Jaakko J. Uusitalo, Helgi I. Ingólfsson, Parisa Akhshi, D. Peter Tieleman, and Siewert J. Marrink. Martini Coarse-Grained Force Field: Extension to DNA. *Journal of Chemical Theory and Computation*, 11(8):3932–3945, 2015.
- [38] Paulo C. T. Souza, Riccardo Alessandri, Jonathan Barnoud, Sebastian Thallmair, Ignacio Faustino, Fabian Grünewald, Ilias Patmanidis, Haleh Abdizadeh, Bart M. H. Bruininks, Tsjerk A. Wassenaar, Peter C. Kroon, Josef Melcr, Vincent Nieto, Valentina Corradi, Hanif M. Khan, Jan Domański, Matti Javanainen, Hector Martinez-Seara, Nathalie Reuter, Robert B. Best, Ilpo Vattulainen, Luca Monticelli, Xavier Periole, D. Peter Tieleman, Alex H. De Vries, and Siewert J. Marrink. Martini 3: a general purpose force field for coarse-grained molecular dynamics. *Nature Methods*, 18(4):382–388, 2021.
- [39] Riccardo Alessandri, Jonathan Barnoud, Anders S. Gertsen, Ilias Patmanidis, Alex H. De Vries, Paulo C. T. Souza, and Siewert J. Marrink. Martini 3 Coarse-Grained Force Field: Small Molecules. *Advanced Theory and Simulations*, 5(1):2100391, 2022.
- [40] Riccardo Alessandri, Jaakko J. Uusitalo, Alex H. De Vries, Remco W. A. Havenith, and Siewert J. Marrink. Bulk Heterojunction Morphologies with Atomistic Resolution from Coarse-Grain Solvent Evaporation Simulations. *Journal of the American Chemical Society*, 139(10):3697–3705, 2017.
- [41] Mark James Abraham, Teemu Murtola, Roland Schulz, Szilárd Páll, Jeremy C. Smith, Berk Hess, and Erik Lindahl. GROMACS: High performance molecular simulations through multi-level parallelism from laptops to supercomputers. *SoftwareX*, 1-2:19–25, 2015.
- [42] Giovanni Bussi, Davide Donadio, and Michele Parrinello. Canonical sampling through velocity rescaling. *The Journal of Chemical Physics*, 126(1):014101, 2007.
- [43] George A. Kaminski, Richard A. Friesner, Julian Tirado-Rives, and William L. Jorgensen. Evaluation and Reparametrization of the OPLS-AA Force Field for Proteins via Comparison with Accurate Quantum Chemical Calculations on Peptides. *The Journal of Physical Chemistry B*, 105(28):6474–6487, 2001.

- [44] H. J. C. Berendsen, J. R. Grigera, and T. P. Straatsma. The missing term in effective pair potentials. *Journal of Physical Chemistry*, 91(24):6269–6271, 1987.
- [45] Djurre H. de Jong, Svetlana Baoukina, Helgi I. Ingólfsson, and Siewert J. Marrink. Martini straight: Boosting performance using a shorter cutoff and GPUs. *Computer Physics Communications*, 199:1–7, 2016.
- [46] Luca Gammaitoni, Peter Hänggi, Peter Jung, and Fabio Marchesoni. Stochastic resonance. *Reviews of Modern Physics*, 70(1):223–287, 1998.
- [47] Thomas Wellens, Vyacheslav Shatokhin, and Andreas Buchleitner. Stochastic resonance. *Reports on Progress in Physics*, 67(1):45–105, 2004.
- [48] Alexander D. Muratov, Anastasia A. Markina, Dmitry V. Pergushov, and Vladik A. Avetisov. Modeling of thermosensitive stereoregular polymers within the coarse-grained force field: Poly(N-isopropylacrylamide) as a benchmark case. *Physics of Fluids*, 33(8):087110, 2021.